

Feed-Forward Control Upgrade of the Deep Space Network Antennas

W. Gawronski

Ground Antennas and Facilities Engineering Section

In order to improve the accuracy of high-rate tracking of NASA's DSN antennas, the position-loop controller has been upgraded with a feed-forward loop. Conditions for perfect and approximate tracking with the feed-forward loop are presented. The feed-forward loop improves tracking performance and preserves wind disturbance rejection properties of the previous closed-loop system.

Pointing accuracy of a proportional and integral (PI) control system for the DSN antennas [1] is satisfactory for slow-tracking antennas but significantly deteriorates when tracking fast-moving objects. In order to improve the tracking accuracy in the latter case, a PI control system has been augmented with a feed-forward loop, as shown with the block diagram in Fig. 1. In this diagram, G_p , G_c , G_f , and G_w denote transfer functions of the antenna's rate loop, PI controller, feed-forward gain, and wind disturbance, respectively; and r is a command, y is output (elevation and azimuth angles), e is tracking error in azimuth and elevation, u is plant input, and w is wind disturbance. The plant transfer function $G_p(\omega)$ is a 2×2 matrix, with elevation and azimuth rates as inputs and elevation and azimuth angles as outputs.

In order to analyze the impact of the feed-forward gain on the closed-loop system performance, the transfer function from the command r and wind disturbance w to the tracking error e was derived. From Fig. 1, one obtains

$$e = r - y \quad (1a)$$

$$y = G_p u + G_w w \quad (1b)$$

$$u = G_f r + G_c e \quad (1c)$$

Assuming $I + G_p G_c$ to be nonsingular and denoting that $G_o = (I + G_p G_c)^{-1}$, from Eqs. (1a), (1b), and (1c), one obtains

$$e = G_o(I - G_p G_f)r - G_o G_w w \quad (2)$$

From the above equation one obtains perfect tracking (i.e., $e = 0$) in the absence of wind disturbances for the feed-forward gain G_f such that

$$G_p(\omega)G_f(\omega) = I \quad (3)$$

In the case of the DSN antennas, the condition (3) can be satisfied in a certain frequency range only. Simply by inspection of the magnitudes of the plant transfer function in Fig. 2(a-d), one can see that for frequencies $0 \leq \omega \leq 2\pi$

rad/sec ($0 \leq f \leq 1$ Hz), the plant transfer function G_p can be approximated with an integrator

$$G_p \cong G_{po} = (j\omega)^{-1} I_2 \quad \text{for } 0 \leq \omega \leq 2\pi \text{ rad/sec} \quad (4)$$

Thus, the feed-forward differentiator

$$G_f = j\omega I_2 \quad (5)$$

will satisfy Eq. (3) in the frequency range $0 \leq \omega \leq 2\pi$ rad/sec. In Fig. 2(a), the diagonal terms of the differentiator transfer function of Eq. (5) are shown with dotted lines. Their inverses (dashed lines) are equal to the plant transfer function, as in Fig. 2 for frequencies up to 1 Hz. The off-diagonal terms of Eq. (5) (transfer functions from elevation command to azimuth position, and from azimuth command to elevation position) should be zero; actually, they are small for frequencies up to 1 Hz, as in Fig. 2(b) and Fig. 2(d).

The closed-loop transfer functions for a system with and without the feed-forward gain are compared in Fig. 3. Figures 3(a) and 3(c) show that for frequencies up to 1 Hz, the system with the feed-forward gain has superior tracking properties when compared with the system without feed-forward gain. This is confirmed by tracking simulations with a trajectory like that in Figs. 4(a) and

4(b). The DSS-13 antenna, with the proportional gain $k_p = 0.5$, and the integral gain $k_i = 1.8$ in azimuth and elevation, was investigated. The tracking errors in elevation and cross-elevation are compared for the antenna with the feed-forward loop (Fig. 5) and without the feed-forward loop (Fig. 6). A significant improvement in tracking accuracy for the system with the feed-forward loop was observed, namely, from 73.1 to 1.4 mdeg in elevation, and from 60.1 to 0.2 mdeg in cross-elevation. However, the high-frequency components of the command are strongly amplified for the system with feed-forward gain when compared with the system without feed-forward gain. This effect can be observed from the transfer function plots in Fig. 3, where the resonance peaks of the system with feed-forward gain are much higher than the ones of the system without feed-forward gain. Also the intensive oscillatory motion in the pointing error plots (see Fig. 5) is observed. As a result, any sharp change in the command may cause excessive vibrations of the antenna.

Despite the increased sensitivity to the command inputs, the disturbance rejection of the antenna with feed-forward gain remains the same as that for the antenna without feed-forward gain. This follows from Eq. (2), where it is shown that the tracking error e due to wind disturbance w is independent of the feed-forward gain G_f . Thus the pointing errors due to wind gust disturbances are comparable with the results obtained for the DSS-13 antenna with the PI controller (see [2]).

References

- [1] W. Gawronski and J. A. Mellstrom, "Modeling and Simulations of the DSS 13 Antenna Control System," *TDA Progress Report 42-106*, vol. April-June, Jet Propulsion Laboratory, Pasadena, California, pp. 204-248, August 15, 1991.
- [2] W. Gawronski, B. Bienkiewicz, and R. E. Hill, "Pointing-Error Simulations of the DSS-13 Antenna Due to Wind Disturbances," *TDA Progress Report 42-108*, vol. October-December, Jet Propulsion Laboratory, Pasadena, California, pp. 109-134, February 15, 1992.

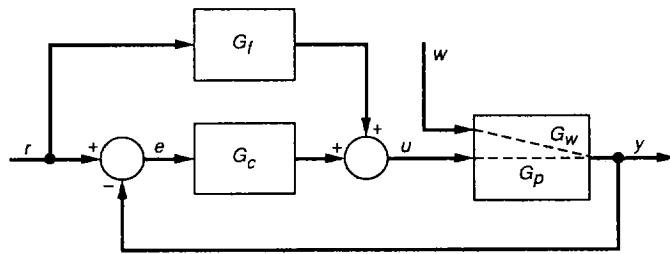


Fig. 1. Antenna control system with the feed-forward loop.

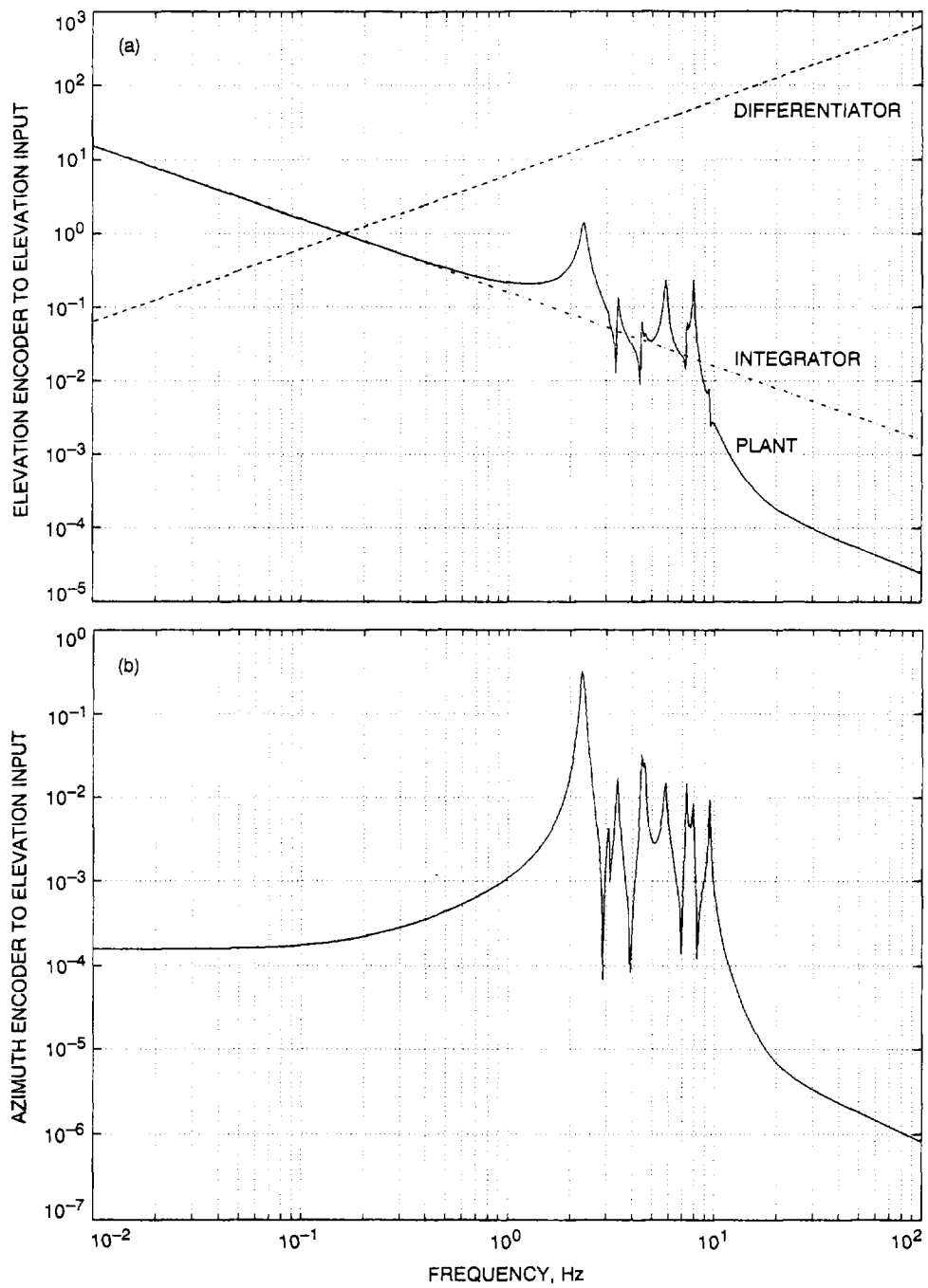


Fig. 2. Transfer functions of antenna rate loop model and of differentiator and integrator: (a) elevation encoder to elevation input; (b) azimuth encoder to elevation input; (c) azimuth encoder to azimuth input; and (d) elevation encoder to azimuth input.

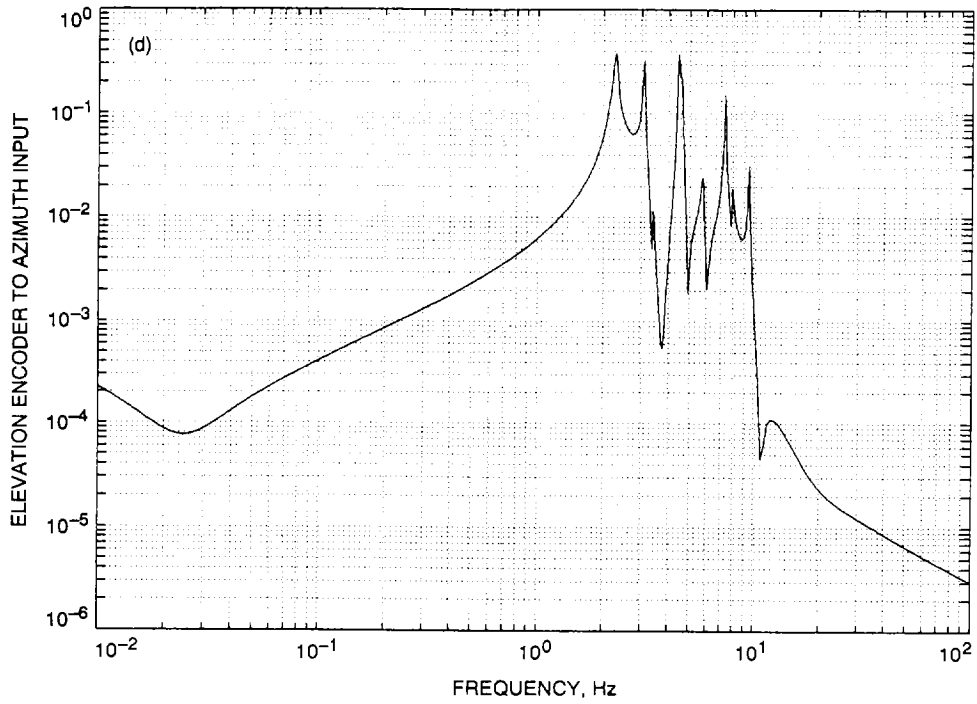
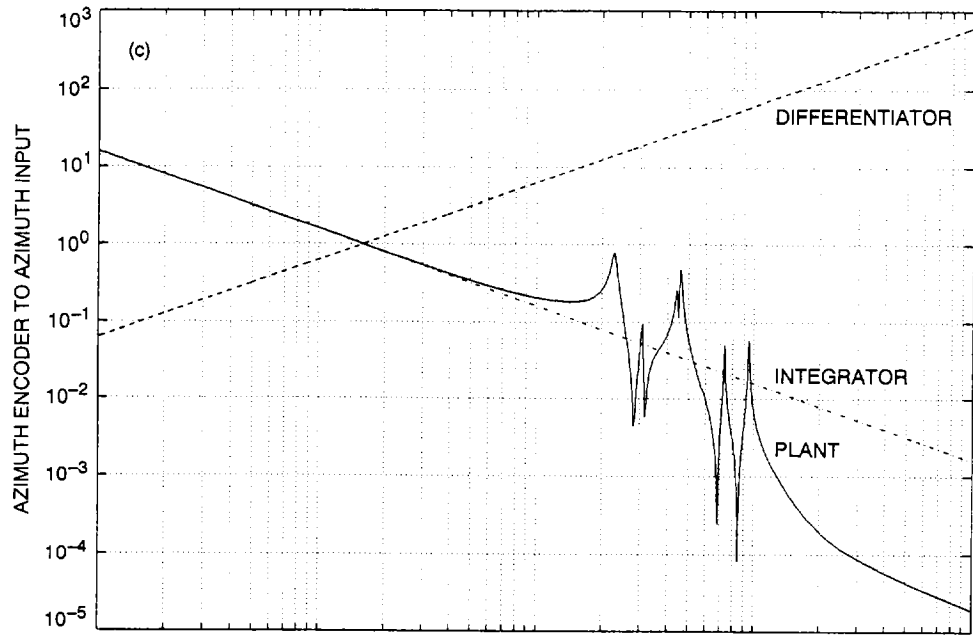


Fig. 2 (contd).

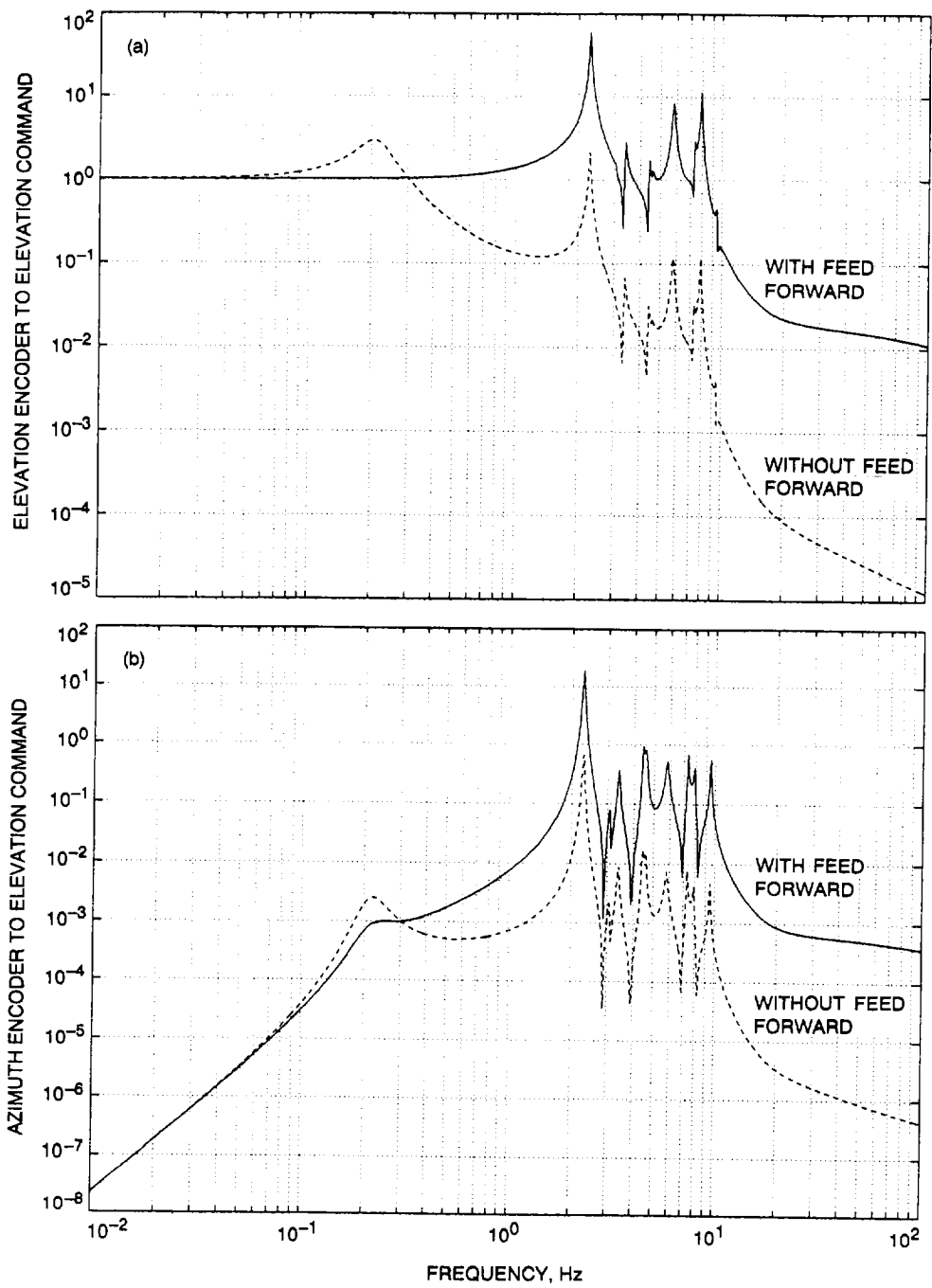


Fig. 3. Closed-loop transfer functions—with feed-forward loop and without feed-forward loop: (a) elevation encoder to elevation command; (b) azimuth encoder to elevation command; (c) azimuth encoder to azimuth command; and (d) elevation encoder to azimuth command.

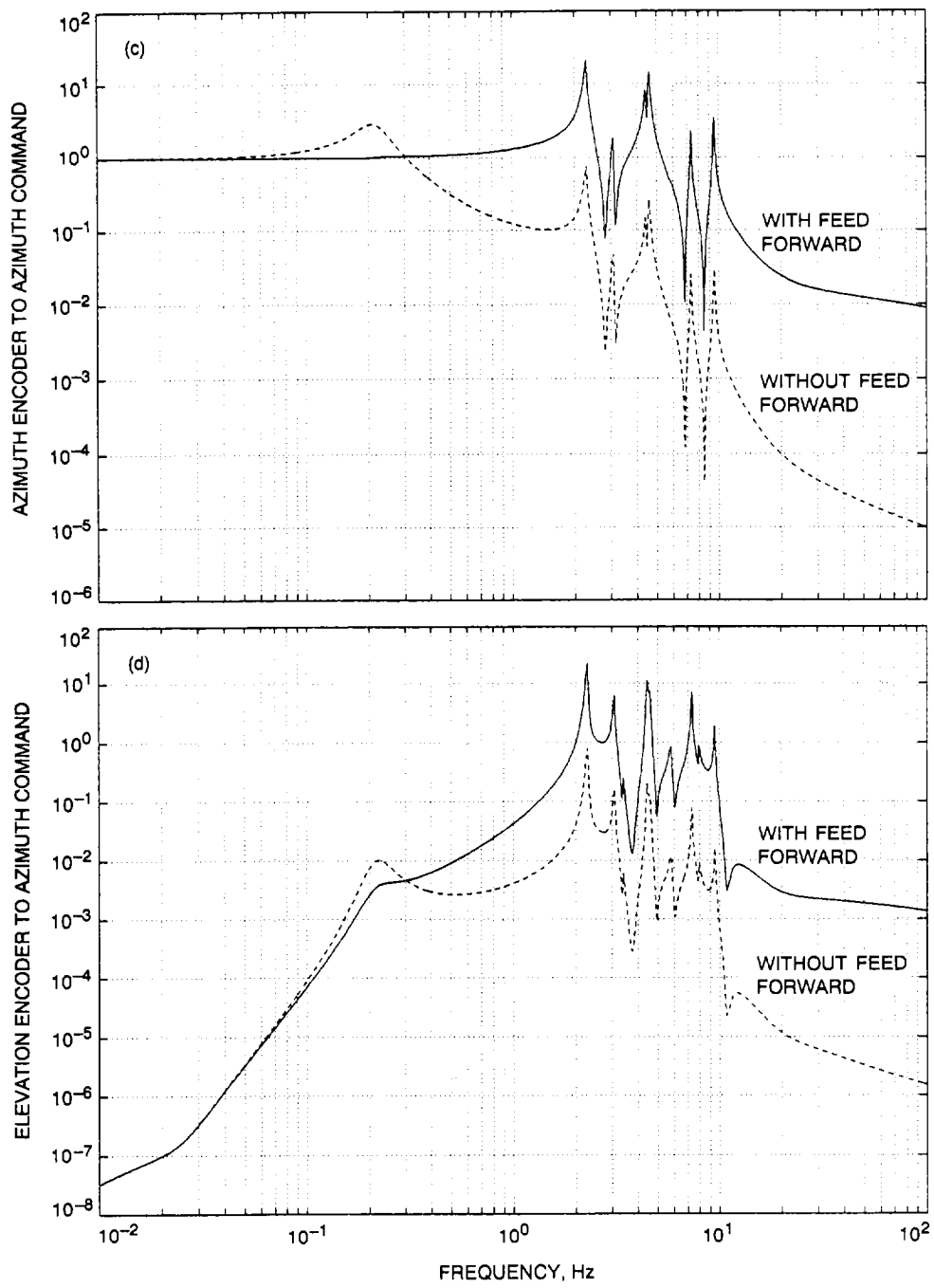


Fig. 3 (contd).

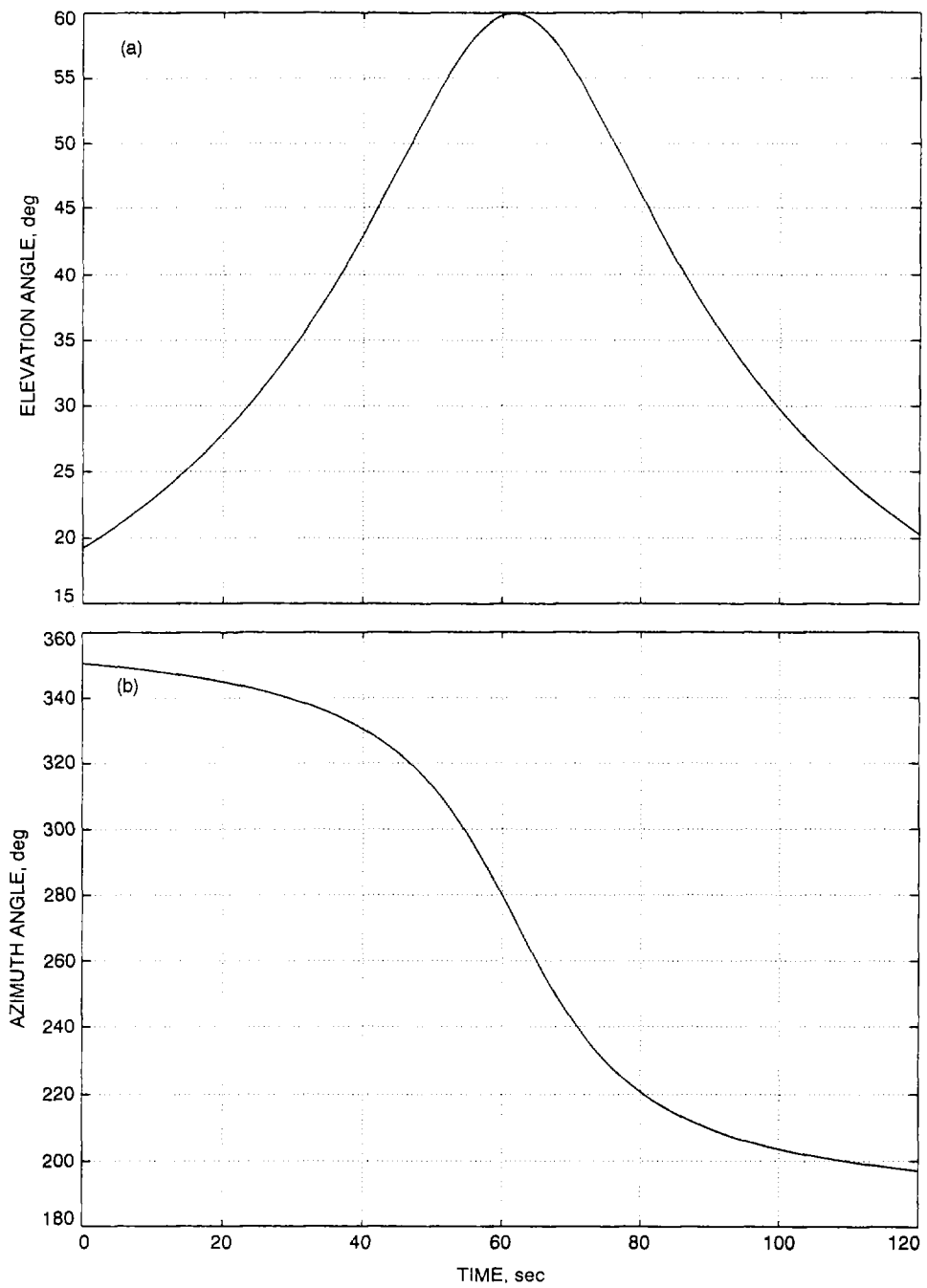


Fig. 4. Trajectory used for simulations: (a) in elevation and (b) azimuth.

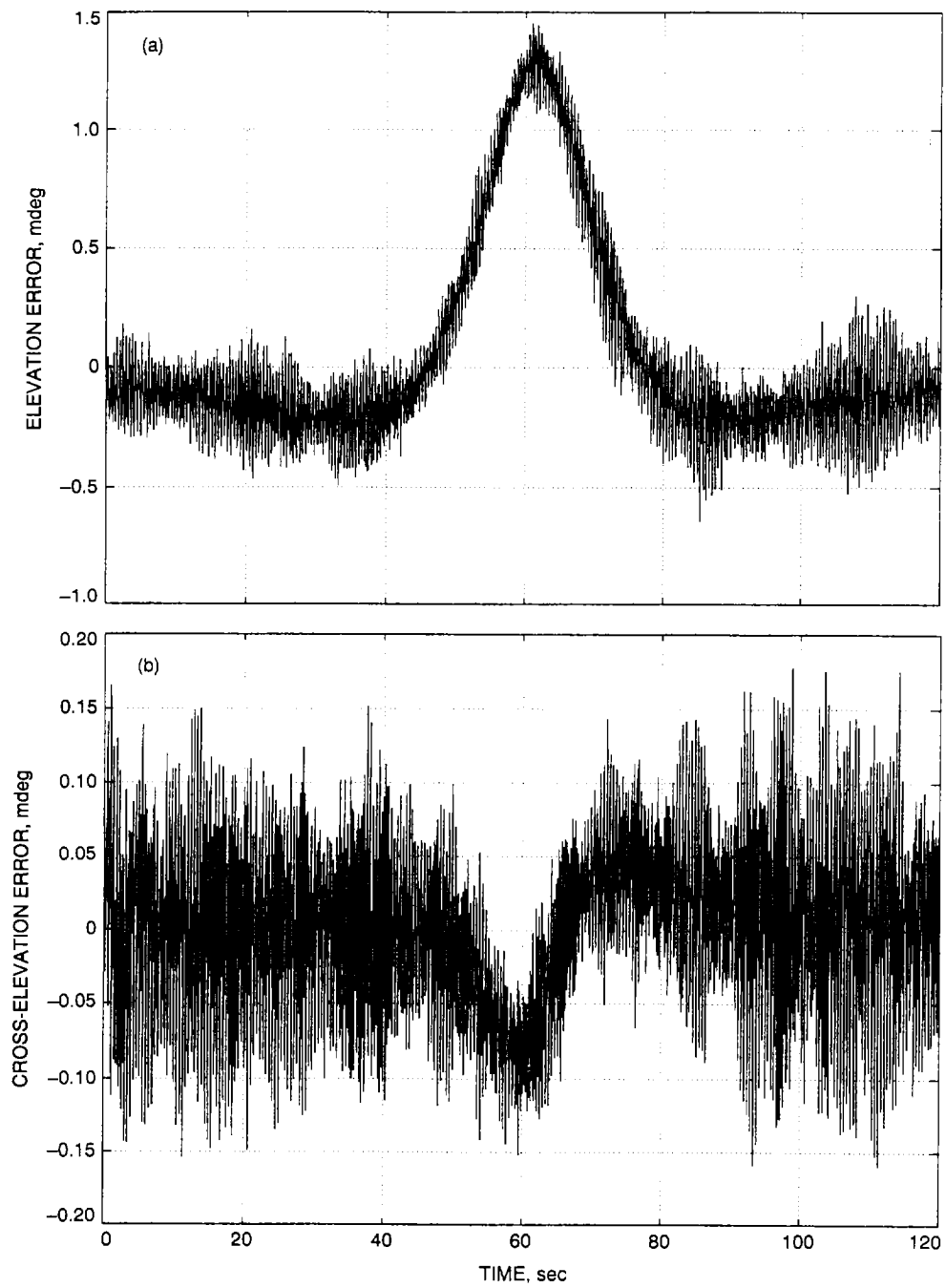


Fig. 5. Pointing errors for the control system with the feed-forward loop: (a) elevation error and (b) cross-elevation error.

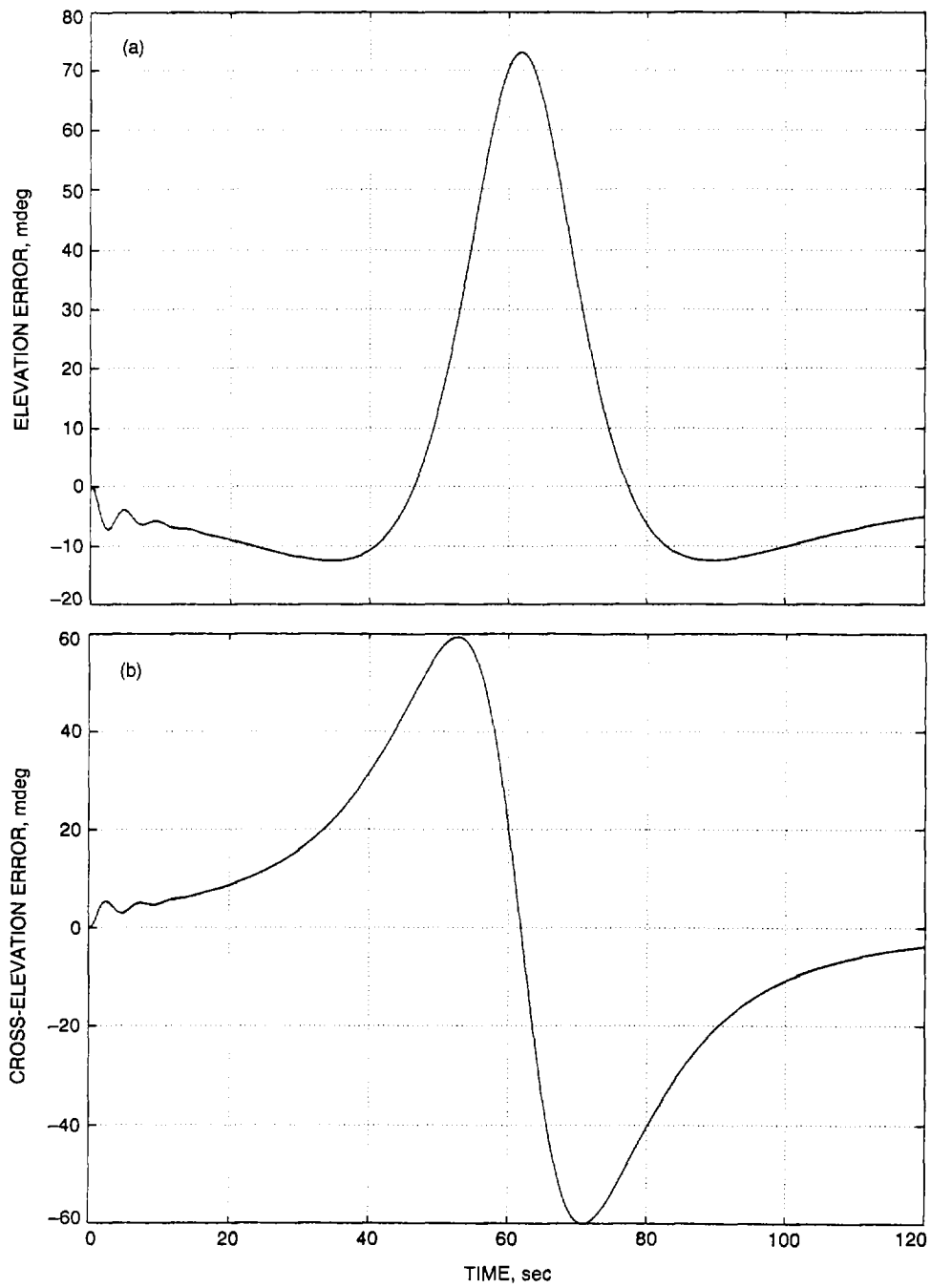


Fig. 6. Pointing errors for the control system without the feed-forward loop: (a) elevation error and (b) cross-elevation error.